Title
TUBULAR PINCH AND TEARING INSTABILITY

Authors
Anderson, Oscar A.
Kunkel, Wulf B.

Publication Date
1969-01-28

UCRL-18415
cy. 2

TUBULAR PINCH AND TEARING INSTABILITY

Oscar A. Anderson and Wulf B. Kunkel

January 28, 1969

LRL
LAWRENCE RADIATION LABORATORY
UNIVERSITY of CALIFORNIA BERKELEY

UCRL-18415
cy. 2

DISCLAIMER

Submitted for publication
to Physics of Fluids

UCRL-18415
Preprint

UNIVERSITY OF CALIFORNIA

Lawrence Radiation Laboratory
Berkeley, California

AEC Contract No. W-7405-eng-48

TUBULAR PINCH AND TEARING INSTABILITY

Oscar A. Anderson and Wulf B. Kunkel

January 28, 1969

TUBULAR PINCH AND TEARING INSTABILITY*

Oscar A. Anderson† and Wulf B. Kunkel

Lawrence Radiation Laboratory
University of California
Berkeley, California

January 28, 1969

ABSTRACT

Theoretical considerations and previous experimental findings with fast tubular (cylindrical sheet) pinch discharges are reviewed briefly. More recent work with magnetic probes as well as streak and Kerr cell photography corroborates that the sheet-current configuration can be sufficiently stable to survive a fair number of pinch oscillations. It is shown, however, that under conditions of high compression the current layer is likely to break up into a set of individual channels because of a resistive instability. The process involves tearing and reconnection of magnetic field lines. Wavelengths and growth rates seem to be in agreement with rough theoretical predictions. The current channels form separate linear pinches, which under certain circumstances disintegrate subsequently by a secondary instability. A generally turbulent behavior results. Tearing is not prevented by superposition of a strong axial magnetic field, again in agreement with theory, although a slight retardation is noted. When deuterium is used in the discharge, neutrons are emitted. Presumably because of the slow rate of reconnection in most of our studies, the neutrons appear mainly during the secondary instability rather than at the time of tearing. These findings are of interest both to astrophysics and to controlled-fusion research.

I. INTRODUCTION

The tubular (cylindrical sheet) pinch has been described before under the name of either "Triax"[1,2] or "Hohlpinch"[3], and some of its stability properties in the limit of infinite conductivity have been discussed at length.[4,5] In this note we therefore review only briefly the principal experimental and theoretical features of this interesting configuration and emphasize those aspects that have not yet been adequately dealt with in the literature. In particular we report on very clear-cut observations of an important instability, the "tearing mode," which occurs here because the plasma has only finite conductivity.[6]

The plasma in this experiment is created in the shape of a hollow cylindrical sleeve by passing a high current through a low-density gas along the annular space between two coaxial return conductors, as indicated in Fig. 1. The configuration thus formed is the simplest type of "hard-core" pinch possible.[7] It differs from other linear "hard-core" stabilized pinch discharges[7-9] in several respects: (a) the current layer is relatively thin, (b) the current density and the plasma density are relatively high, (c) the time scale is relatively short, i.e., the pinch is fromed impulsively (dynamic pinch), (d) the diameter of the inner return conductor (hard core) is relatively large, (e) the inner and outer return currents are not controlled independently but are tightly coupled in a manner that produces self-centering of the discharge channel, and (f) in most of this work no stabilizing axial magnetic field is added.

The trapped and compressed plasma cylinder may be thought of as

resulting from a collision between two magnetically propelled current sheets. One of these is traveling radially inward as in any linear-pinch implosion, while the other is moving radially outward exactly as in the so-called "inverse pinch" experiments.[10,11] Typical streak-camera pictures photographed through a slot in the anode are shown in Fig. 2 to illustrate this behavior. Under certain conditions the sheets will perform a number of distinct "bounces," indicating that the collisions can be fairly elastic and that a relatively stable equilibrium must exist.

II. EQUILIBRIUM

If the configuration has perfect cylindrical symmetry as indicated in Fig. 1, and if all currents are axial (i.e., if there is no axial magnetic field), the condition for equilibrium $dP/dr + (B/4\pi r)d(rB)/dr = 0$ can be integrated directly. It yields the hollow-pinch equivalent of the familiar Bennet condition,

$$I_b^2 - I_a^2 = 4\pi k \int_a^b (n_e T_e + n_i T_i) r dr \equiv 2NkT_{av}, \qquad (1)$$

where N is the total number of particles per unit length of plasma, while I_a and I_b represent the portions of the current that return on the inner and outer conductors respectively.

It is interesting to note that, in principle at least, the energy content of the plasma can here be determined from a simple measurement of currents (or magnetic fields). This possibility arised because in the tubular sheet configuration the plasma pressure exerts a so-called

hoop stress which must be counteracted by magnetic forces. Unfortunately, quantitative inspection reveals that the currents or the fields usually would have to be determined with extreme precision.

Equation (1) demonstrates also that tubular pinches require larger currents than ordinary columnar ones to contain plasma of a given energy content. This is not surprising, of course, since the total plasma perimeter in this configuration is very much larger.

The equilibrium position, i.e., the radius of the cylindrical sheet, depends on the magnetic field distribution. In our experiments the annular discharge chamber was completely surrounded by highly conducting copper or aluminum surfaces so that the net flux of enclosed azimuthal field had to be equal to zero at all times. This means the flux Φ between the inner wall and the surface of zero field had to be exactly equal and opposite to the flux between this surface and the outer wall. If the regions $a \leq r \leq r_1$ and $r_2 \leq r \leq b$ are current free, as sketched in Fig. 1, and if the radius of the $B = 0$ surface is denoted by r_0, this "flux balance" condition can be written as

$$\Phi = 2I_a \ln \frac{r_1}{a} + \int_{r_1}^{r_0} |B(r)|\,dr = 2I_b \ln \frac{b}{r_2} + \int_{r_0}^{r_2} |B(r)|\,dr, \qquad (2)$$

where the regions enclosed by the electrode structure have been neglected.

Suppose now that the flux in the current-carrying region can also be neglected, as in a skin-current approximation, or simply because the entire layer is thin: $r_2 - r_1 \ll b - r_2$. In that case pressure balance

requires that $B(r_1) = B(r_2)$ so that $I_a/I_b = r_1/r_2$ and relation (2) becomes

$$r_1 \ln r_1/a = r_2 \ln b/r_2. \tag{3}$$

In the thin-sheet limit ($x \to 0$) this reduces to

$$r_0^2 = ab. \tag{4}$$

III. STABLE OSCILLATIONS

The initial pinch resulting from the collision of the two current sheets is ordinarily not in exact magnetohydrostatic equilibrium. First of all, as in any rapid implosion, inertial effects tend to cause a certain amount of overcompression (compressive perturbation). And secondly, unless special precautions are taken, an imbalance in the two radial momenta at first will carry the entire plasma sheet inward well beyond the equilibrium position (displacement perturbation). The imbalance arises because normally both mass and current in the outer sheet are larger than in the inner one.[12] The latter defect can be, and in all later work has been, remedied by addition of some external inductance to the outer return circuit to reduce the initial rate of rise of current in the outer plasma sheet (see Fig. 2b).

Inasmuch as these "overshoots" are small they can be considered as perturbations of the equilibrium. Fortunately, as can be readily demonstrated, hard-core pinches are always stable with respect to the two types of perturbations mentioned, provided the conductivity is sufficiently high. In fact, the resulting oscillations, which have been described before,[1,3] may be identified as symmetric and antisymmetric

normal modes of the lowest order, i.e., $k_z = 0$, $m = 0$.[4] We retain the physically descriptive terms "compression" and "displacement" oscillations. Both types of oscillations are easily discernable on the streak photograph shown in Fig. 2a. But the gross behavior of the tubular pinch is also observable by simple electrical measurements. In this context it is expedient to regard the plasma and its container as a circuit element since both layer thickness x and layer position r_0 have a direct effect on the tube impedance. The relationship is best expressed in terms of the effective discharge inductance per unit length, defined as $L \equiv V/\dot{I} = \Phi/I$, where the total current $I = I_a + I_b$. For small layer thickness, $x \ll b - a$, and for small displacements from the equilibrium position, $\xi \equiv 1 - r_0/(ab)^{1/2} \ll 1$, this inductance becomes[13]

$$L \approx L_0 - \frac{x}{2(ab)^{1/2}} - \frac{\xi^2}{L_0}, \tag{5}$$

where $L_0 = (1/2) \ln (b/a)$ represents the value of L for an infinitely thin sheet at $r_0 = (ab)^{1/2}$. Thus we see that small displacements ξ have only a second-order effect on current and voltage of the discharge, whereas variations in the compression, δx, enter linearly.

A. Compression Oscillations

According to the above argument, oscillations of the plasma thickness should be clearly visible by their effect both on the tube voltage and, in the usual circuits, on dI/dt. Figure 3 shows some particularly pronounced cases of such oscillations, which evidently are strongly excited by the initial compression in the first pinch. The periods τ_s

may be directly interpreted as the transit times of compression waves through the pinched plasma:

$$\tau_s \approx x/\overline{\left[(\gamma + 2/\beta)P/\rho\right]^{1/2}}, \qquad (6)$$

where $P = k(n_e T_e + n_i T_i)$ and $\beta = 8\pi P/B^2$ as usual, and the bar denotes a spatial average. More refined analyses of the dynamic behavior of these plasmas for sharp pinch boundaries[3,4] and for distributed currents[14] yield modified expressions but agree with this interpretation in substance.

The persistence of compression oscillations for several periods is evidence of low viscosity and high conductivity in the plasma, and of considerable stability of the configuration. Under favorable conditions, up to eight full cycles have been observed. As had been reported before, in hydrogen and deuterium at pressures below about 0.2 torr, compression oscillations appeared only when the plasma was vigorously preionized by a powerful preheating discharge.[1] Such preparation was necessary in that case for the formation of well-defined current sheets. But even then only two or perhaps three very heavily damped bounces could be seen at low pressure, indicating strong dissipation presumably due to viscosity. Interestingly, as seen in Fig. 4, the full measure of elasticity was readily restored by the addition of a B_z field, clearly demonstrating the reduction of viscosity by a magnetic field. Simultaneously, of course, such a field caused an increase in the bounce frequency, in accordance with Eq. (6).

B. Displacement Oscillations

As pointed out above, small-amplitude displacement oscillations

$d\xi/dt$ have little effect on L and are therefore not discernible in Figs. 3a and b. However, as can be seen from Eq. (2), the individual currents I_a and I_b are affected directly so that a magnetic-field probe sensing B_θ near the outside wall will respond to this plasma motion as well as to the compressions. If, as before, the flux in the current-carrying region can be neglected and if the displacements ξ are small, one finds from Eq. (2):

$$\frac{dI_b}{dt} \approx \frac{dI}{2dt} - \frac{I}{2L_0}\frac{d\xi}{dt} . \tag{7}$$

The probe trace in Fig. 3d shows the superposition very nicly since the two frequencies involved in this case differ approximately by a factor of 2.

The frequency of the oscillations in ξ depends of course on the mass of the plasma cylinder and on the restoring force that holds it in the equilibrium position. The same theoretical studies that treat compressions also describe these displacements in radius and show that the oscillations are indeed stable provided that the cylindrical symmetry is maintained, i.e., if the perturbations have neither azimuthal nor axial dependence.[4,14] A highly simplified analysis, good for crude quantitative estimates, yields as an expression for the frequency:[13]

$$\omega^2 = \frac{I^2}{N_i m_i abL_0} , \tag{8}$$

where $N_i m_i$ denotes the mass per unit length of the plasma. It is seen

that ω increases with I, which is indeed observed.

C. Observation of Stable Oscillations

In principle, ω could be used to "weigh" the plasma, whereas the bounce time τ_s yields the speed of sound. In actuality the latter gives reasonable results that are consistent with other data such as the observed plasma thickness and pressure. The frequency ω, on the other hand, is often too low by a factor of 2 or more. This is too much to be accounted for by an uncertainty in the mass and is perhaps caused by small deviations from the cylindrical symmetry that was assumed in the derivation. It is, for instance, conceivable that end effects result in slight deviations from axial uniformity and thus k_z would not be zero but small. Such a feature can well remain undetected by our photographic or magnetic-probe diagnostic technique, but it can have a profound effect on the frequency of displacement oscillations. Compression oscillations have been studied in a variety of experimental tubes of different shapes and sizes, at various pressures, in different gases, and over a range of power levels.

Current distributions were determined, as previously reported, with the help of a set of movable magnetic-field probes. More recently, gross features of the discharge were observed with streak photography through the anode, such as shown in Fig. 2. Stereoscopic photography was used to verify that the light emission seen did indeed originate from a cylindrical region in the gas rather than from some luminosity on one of the electrodes. Occasionally the line profile of the H_β emission was determined as a check on the plasma density, and in deuterium discharges the production of neutrons was recorded.

In general, these additional measurements simply corroborated those reported before,[1,3] as far as stable oscillations are concerned. Compression oscillations, as shown in Fig. 3, are most pronounced and most reproducible in light gases at moderately high initial pressures (0.3 to 1.0 torr) and with modest currents per unit length of circumference ($B_\theta \approx 10^4$ G). These conditions correspond to pinched plasma densities in the 10^{17} cm^{-3} range and temperatures between 10 and 30 eV. The temperatures agree rather well with those inferred from the resistivity, i.e., from the voltage across the terminals at peak current. We therefore reiterate our previous conclusion: under mild compression the tubular pinch is sufficiently stable to execute several normal-mode oscillations about its equilibrium configuration without the help of any longitudinal stabilizing field.

However, when the current density is raised, or when the gas density is reduced, the duration of these stable oscillations decreases markedly. At the same time the appearance of various symptoms, such as a sudden increase in discharge impedance or the emission of bursts of neutrons when deuterium is present, point to the onset of instabilities. Figure 4 shows some good examples of the corresponding oscillographic signals.

IV. INSTABILITIES

A. Infinite-Conductivity Modes

In the outer regions of the tubular pinch the curvature of the magnetic field is obviously unfavorable, so that the configuration is naturally subject to ordinary hydromagnetic instabilities. It may

therefore seem surprising, at first sight, that the plasma can survive many compression oscillations without the help of an axial field to provide stabilizing shear. The explanation is found in the fact that the radius of curvature of our cylindrical sheet pinch is always very large compared with its thickness. As a result even the fastest unstable mode has a growth rate slow compared with the frequencies of pinch oscillations.

The stability analysis of Newcomb and Kaufman[5] is restricted to cases with $B_z \neq 0$ and, moreover, is concerned with threshold criteria rather than with growth rates. The paper by Lehner[4] gives growth rates, but these are unrealistically large because only infinitesimally thin skin currents are assumed. For our distributed current and gentle curvature a very adequate estimate of the maximum growth rate p can be obtained from the analogy of the interchange instability driven by a gravitational field. Substitution of line-curvature and gradient-B effects for the graviational acceleration $g = 2P/\rho r$, leads to the result

$$p^2 \approx \frac{2P}{\rho r} \frac{d \ln \rho}{dr} \approx \frac{4x/r_0}{(\gamma + 2/\beta)\, \tau_s^2} . \qquad (9)$$

Except for a small correction caused by compressibility the first of these expressions agrees with one given by Kadomtsev.[15] It may also be deduced from a relation carefully derived by Newcomb for gravitational MHD instabilities, using a local approximation.[16] The second expression is gotten by substitution of τ_s from Eq. (6) with the assumption that P/ρ is roughly constant throughout the plasma and by

approximating $r \approx r_0$ and $d(\ln \rho)/dr \approx (r_2 - r_0)^{-1} \approx 2/x$. Since in our experiments we invariably deal with $x < 0.05 r_0$ it is not surprising that we should indeed find $p \ll 1/\tau_s$. In fact, p is sometimes so small that interchange flutes could not possibly develop before the discharge current reaches its maximum value.

The question now arises whether the observed symptoms of instability are caused at all by infinite-conductivity modes such as discussed above. The experimentally obtained appearance-times of the neutron bursts do not agree too well with Eq. (9). Furthermore, it had been noted long ago[1] and has been repeatedly confirmed that the addition of longitudinal magnetic fields, which should have pronounced stabilizing effects on the interchange mode, caused only minor retardation of the instability onset (see Fig. 4). It is thus evident that the phenomenon responsible for the disruption of the tubular pinch is of a different character. The most likely process in this case is the resistive tearing of the current sheet. In the following we present evidence that under strong compression the Triax discharge is indeed destroyed by this finite-conductivity mode.

B. Resistive Tearing Mode

Consider the projection of a general sheared field onto the plane of the paper, as illustrated in Fig. 5a. This could represent the magnetic lines in our sheet pinch, even if an axial stabilizing field is superimposed. Finite resistivity allows flux to link across the (dashed) "null" plane so that closed-loop patterns can develop as shown in Fig. 5b. Tearing is then caused by the attraction of parallel

currents (normal to the plane of the paper) so that the current layer goes over into an array of filaments meeting the Bennet pinch condition. This mode has been observed in theta pinches with reverse trapped field,[17,18] and a similar effect must be responsible for the destruction of current sheets at low density.[19]

For visual detection of tearing in the tubular pinch it was considered desirable to view the entire discharge end-on. A large diameter (a = 15 cm, b = 25 cm) 20-cm long Triax tube was therefore provided with a semitransparent (i.e., perforated) anode backed by a glass plate to hold the vacuum. A six-channel Kerr-cell framing camera was used to photograph the plasma at predetermined intervals. The distance between camera and discharge tube was 30 ft to reduce the parallax. Unfortunately, the light emitted by hydrogen or deuterium was too weak to give usable records, so that helium and argon had to be used for this study. Some examples are shown in Fig. 6. The breakup into a set of strands is clearly visible.

The individual filaments are, of course, expected to be unstable again since they are ordinary linear pinches. This is indeed seen to be the case here in the helium pictures. The apparent stability of the argon filaments seemed puzzling at first. These initial results, augmented by observations with a single magnetic probe, have been briefly reported on before.[20] Stereoscopic photographs revealed that in argon the strong luminosity originated from regions near the electrodes only, so that the optical observations could not give us accurate information about the behavior of the plasma in the body of the discharge. Evidently the only reliable diagnostic technique with argon

involved the use of multiple magnetic-field probes. It was hoped that with helium the probe measurements could be correlated with some of the framing camera results; this method was particularly useful in establishing the wavelength of the instability.

The investigation was thus continued with the help of a set of seven movable probes which were inserted through the ring-shaped anode at 15-deg intervals. The magnetic field could in this way be surveyed along 90 deg of the plasma perimeter. Quite understandably, it was found that these probes had to be positioned far from the compressed plasma to prevent interference with the discharges. For instance, when the probes were tilted to coincide with the equilibrium position of the pinch, the current sheet showed a tendency to tear into 12 channels and the signals had the same polarity every time. Such behavior is an indication that the instability was influenced by the immersed objects. No such correlation was ever seen when the probes were kept near the outer insulator.

A good way to measure the growth of the tearing mode in the cylindrical sheet pinch consists of observing the development of radial components of the magnetic field (see Fig. 5b). Therefore, all seven probes were at first oriented to sense B_r. In the case of helium, which had shown distinct channeling of the discharge also in the stereoscopic framing pictures, direct comparison could be made, as displayed in Fig. 7. While tearing develops, the B_r signals grow gradually except at points where the perturbation has a node. From a large number of such records approximate exponentiation times and wavelengths can be deduced and these agree well with the optical data. In Fig. 8 we plot

the dependence of the e-folding time on the initial gas pressure when all other discharge parameters are held constant.

Quantitative comparison with the theory developed by Furth and coworkers[6] is difficult at this stage for the following reasons:

(1) The relevant parameter in the theory $S \equiv \tau_R/\tau_H$ depends critically on the sheet thickness x as well as on density and temperature. These quantities have not been determined with sufficient accuracy. In cases where fairly good estimates are available, based on optical observations, the value of S is not very large, so that numerical calculations must be used. Furthermore, the stabilizing effect of the conducting walls must be taken into account as well as the curvature of our cylindrical configuration. Some numerical calculations for our experimental arrangement have recently been carried out,[21] but not for enough cases to match all our data. We mention in passing here only that these calculations indeed predict growth rates considerably smaller than those computed for the long-wavelength limit, $kx \ll 1$, in Ref. 6.

(2) Conditions, such as the value of B_θ, change during the development of the instability, so that true exponential growth of the perturbations is not really expected.

(3) Finally, when the B_r signals are large enough to be clearly observable the amplitudes are very probably in the nonlinear domain, to which the theory does not really apply.

The relationship between our observations and the theory is thus primarily of a qualitative nature. Nevertheless it is interesting to compare the pressure dependence shown in Fig. 8a with predictions based

on the theory for constant field and large values of S. In that case the fastest growth time is given by[6]

$$\tau \approx \tau_R S^{-1/2} = (\tau_R \tau_H)^{1/2} \sim (\rho^{1/2} T^{3/2} x^3/B)^{1/2},$$

where τ_R is the resistive diffusion time and τ_H is the Alfven wave transit time for the sheet pinch of thickness x. With pressure balance, $\rho T \sim B^2$, and mass conservation $\rho x \sim P_0$, where P_0 stands for the initial pressure, this becomes $\tau \sim P_0^{3/2} T^2/B^3$. It is seen that the observed behavior is consistent with this relation only if $T^2 B^3$ is nearly invariant. On the other hand, it is worth mentioning that the computations for our cylindrical configuration[21] yield maximum growth rates for wave numbers given by m between 5 and 8 (for values of S between 10 and 100) in rather good agreement with the experimental findings.

Figure 7 also shows violent fluctuations of B_r at the time the secondary instability sets in, i.e., when the individual channels become hydromagnetically unstable. The time of onset of this phase is also plotted in Fig. 8. Surprisingly, the secondary (pinch) instability never shows up early. It seems to require some minimum current regardless of how low the initial pressure is or how rapidly the tearing develops. The increase in discharge impedance that is indicated by the sudden increase in voltage is invariably coincident with the onset of this secondary instability.

In the case of low-pressure argon, where the framing camera had shown channeling without secondary instabilities, the probes indicated that far from the electrodes tearing was very weak, if noticeable at all. Evidently electrode effects enhance or overemphasize the channeling

action. The tearing in the body of the plasma may be suppressed because of the large gyroradii or because the value of S is always too small.

V. TRAPPED FIELDS AND NEUTRON PRODUCTION

A. Trapped B_θ

Although no photographs could be taken, some qualitative studies with deuterium were particularly interesting because of the familiar connection between instabilities and neutron emission. When deuterium is used the sudden increase in voltage is always accompanied by a burst of neutrons. We know now that this is caused by the usual instability of the filamentary secondary pinches. Figure 9a shows a good example at 50 mtorr pressure and high power, including half a cycle of preheating current, and B_r probes indicate rapid growth of channeling. This is one of a large number of tests intended for the study of preheating effects on the plasma and its tearing mode. Notice that the preheating current is in the same direction as the main compression current.

When the preheating current is allowed to ring through two full cycles, as sketched in Fig. 9b, the plasma behavior is quite different. First of all, the voltage now indicates several pinch oscillations which were absent before. This means the plasma must have good conductivity, and presumably it has imbedded a certain amount of magnetic flux, some of which must be in the reverse direction. This seems to be important. The pinch oscillations disappear after a few cycles and a small burst of neutrons is detected simultaneously. This, however, is not yet our usual secondary instability. The latter appears more than 0.5 μsec

later and is accompanied by a much larger neutron production. The magnetic probes this time give no evidence of development of large B_r components until shortly before the onset of the secondary instability. It has been suggested[22] that a relatively fast short-wavelength resistive instability may develop here internally which produces some neutrons and allows the inner trapped reversed fields to relax before the general tearing takes over. The temporary fine-grain turbulence is then the cause for disappearance of the regular pinch oscillations. It does not seem likely that a long-wavelength tearing can occur without being detected by the B_r probes.

B. Trapped B_z

The theory of resistive instabilities predicts that tearing should occur even if the magnetic field does not have a neutral surface as in the pure reversed-field sheet pinch described so far. Indeed, it had never been possible to stabilize our tubular pinches by shear, i.e., by simply adding an axial magnetic field B_z. To verify that the instability consisted of channeling even in this case, the multiple-probe experiments were repeated with a superimposed uniform B_z field with initial values up to 3 kG.

To get an idea of the plasma structure under such conditions, field surveys were made in low-pressure deuterium discharges of about 2×10^6 A peak current. In this case both $B_z(r,t)$ and $B_\theta(r,t)$ were recorded. Some results on B_z are plotted in Fig. 10. The data start near the outer insulator and extend through the current layer but do not reach all the way to the inner wall. The initial field here was 2 kG. Partial trapping and compression to 8 kG at $t = 1$ μsec is clearly seen. The

instability becomes visible at about 1 μsec. Figure 11 shows a similar plot of B_θ which reaches 10 kG outside the layer and reverses sign somewhere inside the plasma. Several pinch oscillations are visible. Calculations give $\beta \approx 0.3$, $kT \approx 20$ eV, and $\tau_R \approx 50\tau_H$. The observed e-folding time of the instability is about 0.2 μsec.

Measurement of $B_r(t)$ near the outer wall showed growth as before for all values of $B_z(0)$. A set of observations of voltage, neutrons, B_r near the wall, and ΔB_z near the center of the layer for a variety of initial values of B_z is reproduced in Fig. 12. It is seen that B_z, even when it dominates the pressure balance, has little effect on the tearing, just as predicted by theory for $\tau_R/\tau_H \gg 1$. The field is seen to be trapped and compressed until the instability develops. The voltage rises and neutrons make their appearance whenever the secondary instability sets in. The only positive effect of B_z is a slight retardation of this secondary instability and a reduction of the neutron output by about a factor of 2.

VI. CONCLUSION

Cylindrical sheet pinches have been shown to be sufficiently stable against ordinary hydromagnetic perturbations to survive a fair number of pinch oscillations. Under conditions of high compression, however, they are likely to tear into a set of filamentary pinches because of a resistive instability. This instability cannot be suppressed by a strong axial magnetic field. These findings corroborate theoretical predictions and have an important bearing on the concepts of magnetic confinement in general and on the prospects for shear

stabilization in particular. The process of line-reconnection also, of course, plays an important role in astrophysical phenomena[23,24] and in space science,[25] but in these cases the mechanism may often be collisionless rather than resistive.

ACKNOWLEDGMENTS

We wish to thank, above all, H. P. Furth for his constant interest and support, valuable advice, and many stimulating discussions. Thanks are also due to C. M. Van Atta for his support of the work, and to W. R. Baker for many good ideas, and to E. B. Hewitt and M. R. Gray for help with the experiments.

FOOTNOTES AND REFERENCES

*Work done under the auspices of the U. S. Atomic Energy Commission.

†Lawrence Radiation Laboratory, Livermore, Calif.

1. O. A. Anderson, W. R. Baker, J. Ise, Jr., W. B. Kunkel, R. V. Pyle, and J. M. Stone, in Proceedings of the Second United Nations International Conference on the Peaceful Uses of Atomic Energy (United Nations, Geneva, 1958), Vol. 32, p. 150.

2. D. J. Rose and M. Clark, Jr., Plasma and Controlled Fusion (M.I.T. Press and John Wiley and Sons, New York, 1961), p. 368.

3. G. Lehner, Z. Naturforsch. 16a, 548 (1961).

4. G. Lehner, Z. Naturforsch. 16a, 700 (1961).

5. W. A. Newcomb and A. N. Kaufman, Phys. Fluids 4, 314 (1961).

6. H. P. Furth, J. Killeen, and M. N. Rosenbluth, Phys. Fluids 6, 459 (1963).

7. S. A. Colgate and H. P. Furth, Phys. Fluids 3, 982 (1960).

8. P. H. Rebut and A. Torossian, J. Nucl. Energy, Pt. C, 5, 133 (1963).

9. K. L. Aitken, R. J. Bickerton, P. Ginot, B. A. Hardcastle, A.Malein, and P. Reynolds, J. Nucl. Energy, Pt. C, 6, 39 (1964).

10. O. A. Anderson, H. P. Furth, J. M. Stone, and R. E. Wright, Phys. Fluids 1, 489 (1958).

11. G. C. Vlases, Phys. Fluids 7, 1358 (1964).

12. This effect is naturally more pronounced in tubes with large ratios b/a. In that case it can lead to difficulties by driving the hot plasma in the first inward excursion all the way back to the inner insulator.

13. W. B. Kunkel, A Simple Analysis of the Tubular Pinch Discharge, Lawrence Radiation Laboratory report UCRL-9311, July 25, 1960 (unpublished).

14. S. Fisher, Some Calculations on the Triax Pinch Device, Lawrence Radiation Laboratory report UCRL-9344, August 9, 1960 (unpublished).

15. B. B. Kadomtsev, Soviet Phys.-JETP 37, 780 (1960).

16. W. A. Newcomb, Phys. Fluids 4, 391 (1961).

17. H. A. B. Bodin, Nucl. Fusion 3, 215 (1963).

18. J. Benford, R. H. Lovberg, and G. B. F. Niblett, Phys. Fluids 11, 218 (1968).

19. M. Alidières, R. Aymar, P. Jourdan, F. Koechlin, and A. Samain, Plasma Physics 10, 841 (1968).

20. O. A. Anderson, Bull. Am. Phys. Soc. 9, 328 (1964).

21. J. Killeen, in Controlled Thermonuclear Research Semiannual Report, Lawrence Radiation Laboratory report UCRL-12028, July 1964 (unpublished).

22. H. P. Furth, Plasma Physics Laboratory, Princeton University, private communication.

23. J. W. Dungey, Cosmic Electrodynamics (Cambridge University Press, 1958), pp. 98-102.

24. P. A. Sturrock, in Structure and Development of Solar Active Regions, O. Kiepenheuer, ed. (Reidel, Holland, 1968), p. 471.

25. R. H. Levy, H. E. Petschek, and G. L. Siscoe, AIAA J. 2, 2065 (1964).

FIGURE LEGENDS

Fig. 1. Tubular pinch geometry, current, and magnetic field.

Fig. 2. Streak photographs of typical discharges viewed through radial slit in anode. (a) Showing both displacement and compression oscillations. (b) Balanced conditions, i.e., displacement oscillations are minimized. The current reached its maximum at 2.5 μsec.

Fig. 3. External electric observables of a typical well-behaved tubular pinch discharge. Conditions were: a = 2.5 cm, b = 5 cm, length 100 cm, filling P_0 = 0.5 torr deuterium, power supply C = 45 μF, V = 20 kV.

Fig. 4. Current, voltage, and neutron signal for discharges with and without longitudinal magnetic field. Conditions as in Fig. 3 except P_0 = 0.1 torr and plasma was preheated.

Fig. 5. Magnetic field lines in tearing mode, projected onto plane normal to the direction of the current. (a) Unperturbed. (b) After some reconnection has taken place.

Fig. 6. Framing camera photographs of tubular pinch discharges taken through a transparent anode, for various gas fillings. Conditions were: a = 7.5 cm, b = 12.5 cm, length 15 cm, C = 85 μF, V = 18 kV, current peak at 2.3 μsec.

Fig. 7. Framing camera photographs and B_r signals with helium at 125 mtorr pressure. Note that visible tearing coincides with growing B_r signals, and very irregular behavior of B_r accompanies secondary instability. Tube and power supply were the same as in Fig. 6.

Fig. 8. Instability time scales in helium at various pressures. Tube and power supply were the same as in Figs. 6 and 7. Error bars indicate uncertainty in determination of best fitting exponential.

Fig. 9. Tube voltage, neutron yield, and B_r-probe signals for 1 and 4 half-cycles of preheating current. Conditions were: tube same as in Fig. 6, filling $P_0 = 0.05$ torr deuterium, main bank C = 340 μF, V = 18 kV.

Fig. 10. Plot of $B_z(r,t)$ showing compression--and later on, fluctuation --of a superimposed axial field. Other conditions same as in Fig. 9a.

Fig. 11. Plot of $B_\theta(r,t)$ for the same discharge as that in Fig. 10.

Fig. 12. Oscillograms of neutron yield, voltage, $B_r(r \approx b)$ and $\Delta B_z(r \approx r_0)$ for various initial values of B_z. Other conditions are as in Fig. 10.

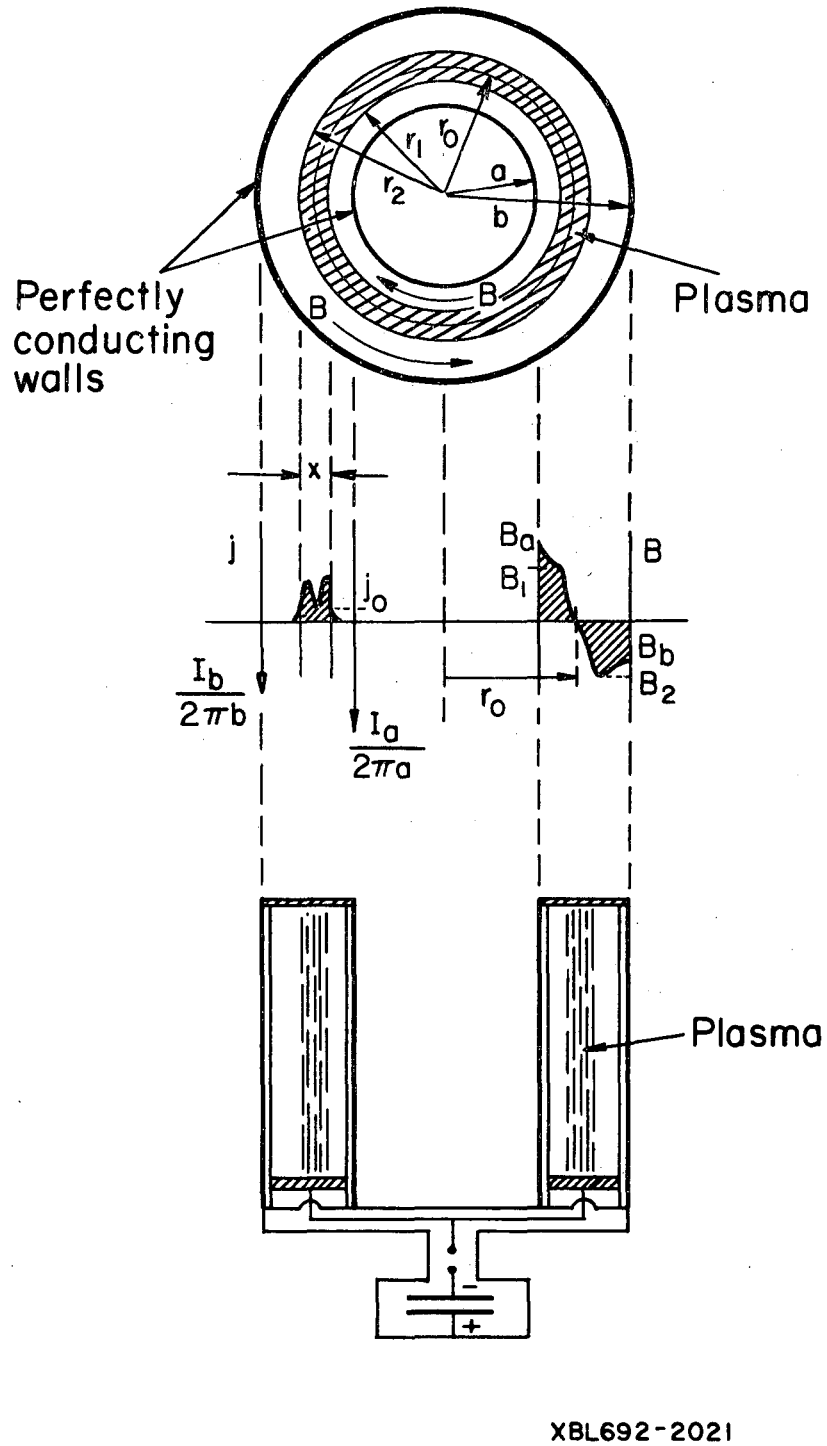
Perfectly conducting walls
Plasma
r_1
r_0
r_2
a
b
B
B
x
j
j_0
B_a
B_1
B
B_b
B_2
r_0
$\frac{I_b}{2\pi b}$
$\frac{I_a}{2\pi a}$
Plasma
XBL692-2021

Fig. 1

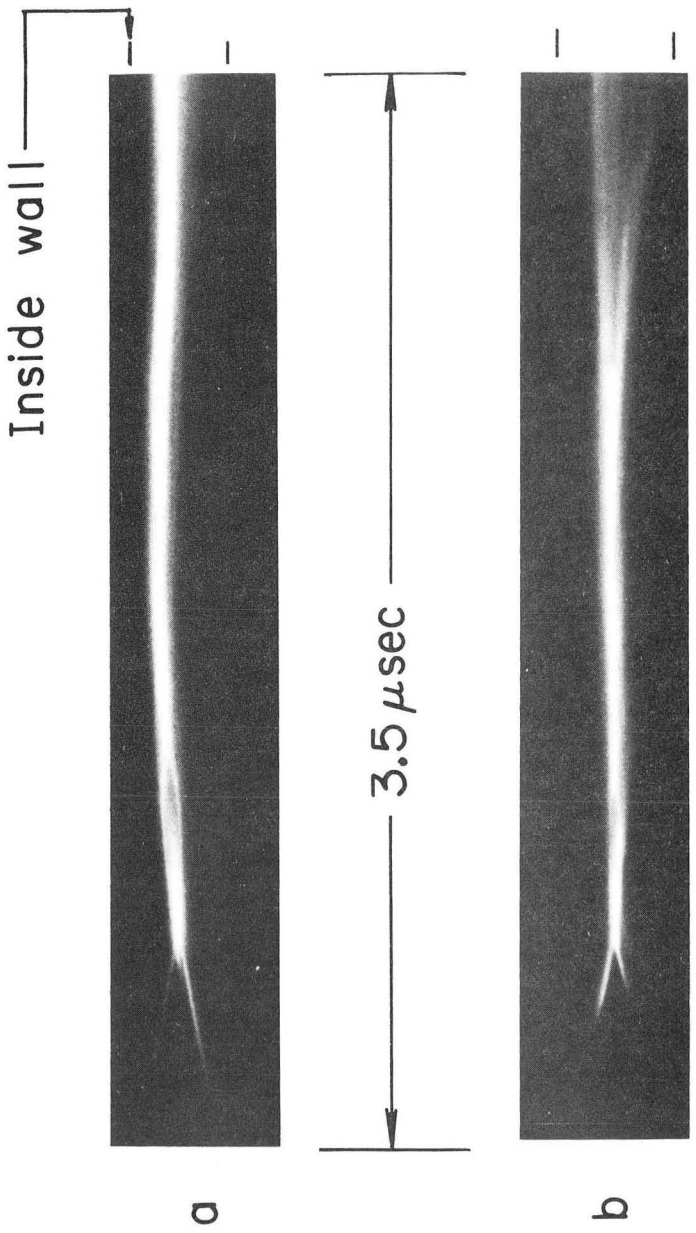

XBB 692-1391

Fig. 2

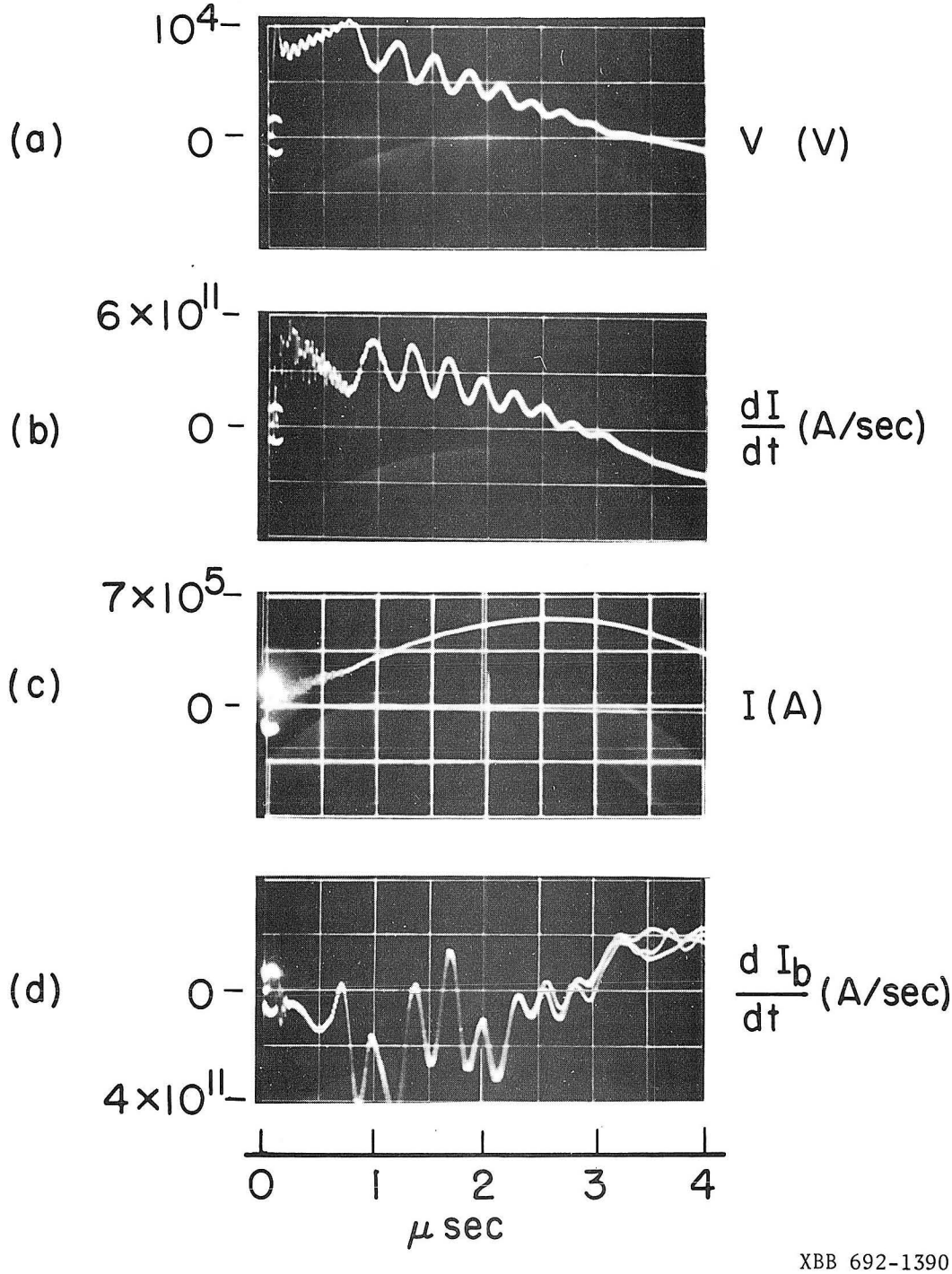
(a)
10^4
0
V (V)
(b)
6×10^{11}
0
$\frac{dI}{dt}$ (A/sec)
(c)
7×10^5
0
I (A)
(d)
0
4×10^{11}
$\frac{d\,I_b}{dt}$ (A/sec)
0
1
2
3
4
μ sec
XBB 692-1390

Fig. 3

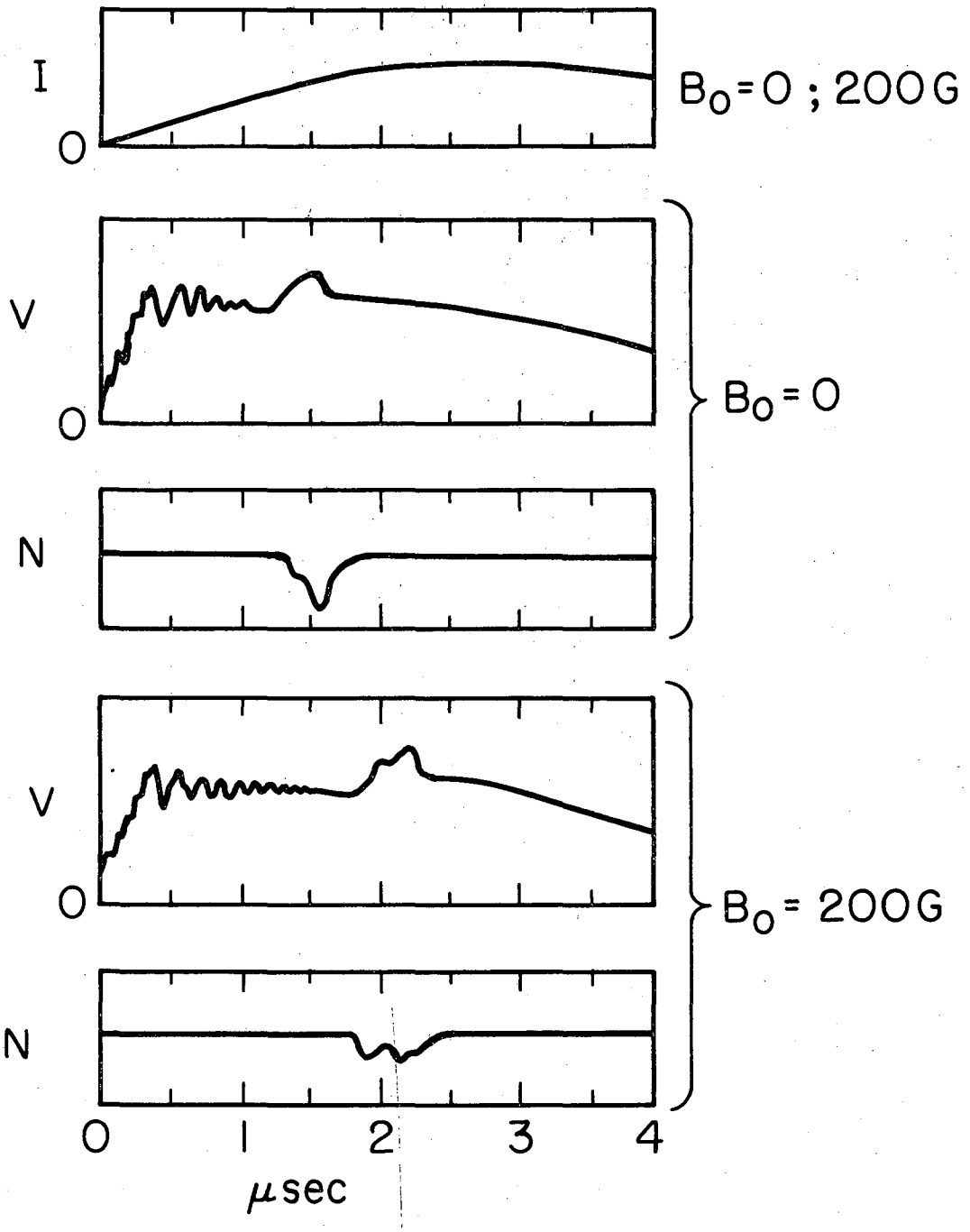

XBL692-2022

Fig. 4

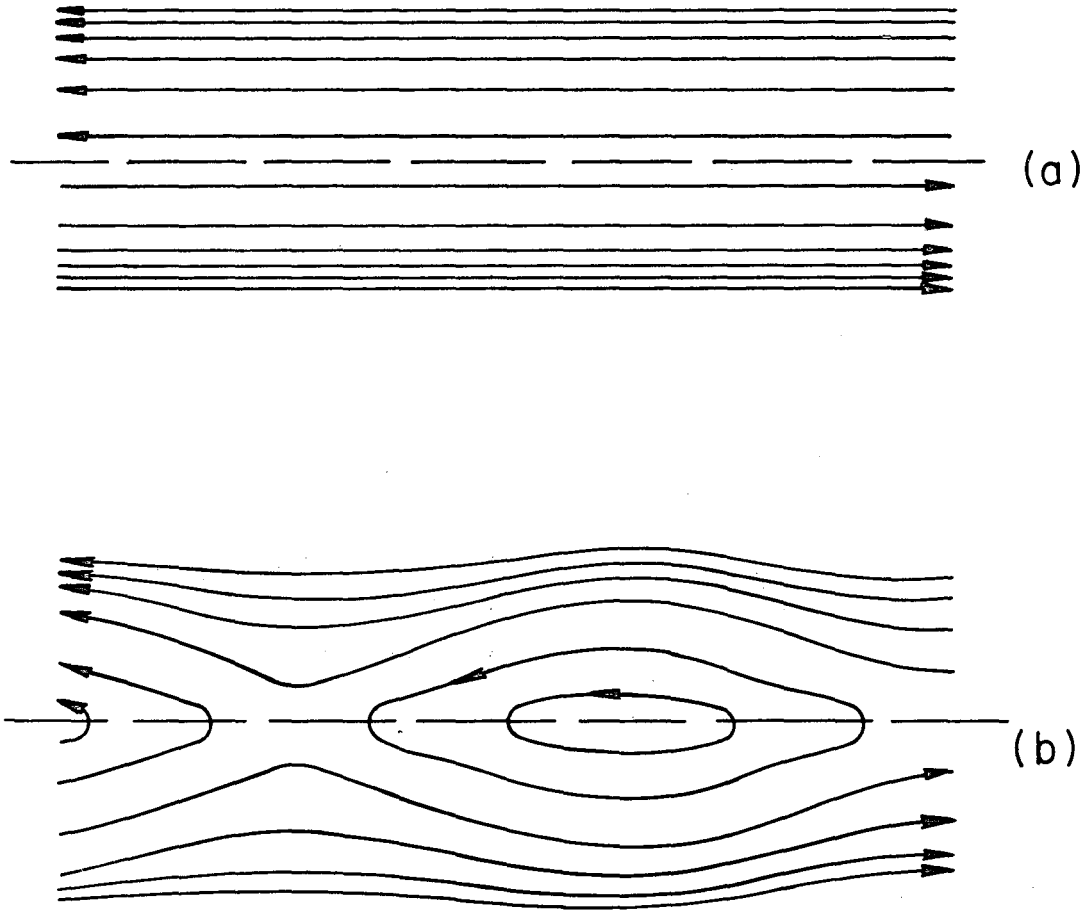

XBL692-2023

Fig. 5

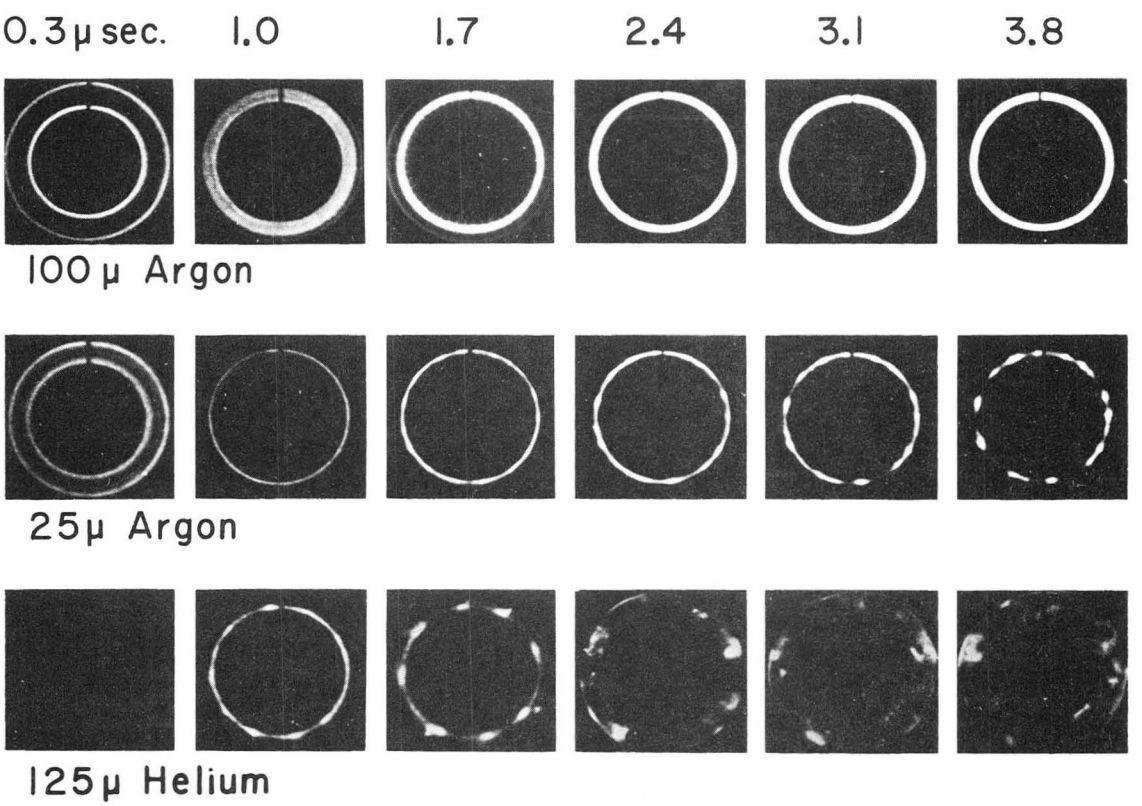

Fig. 6

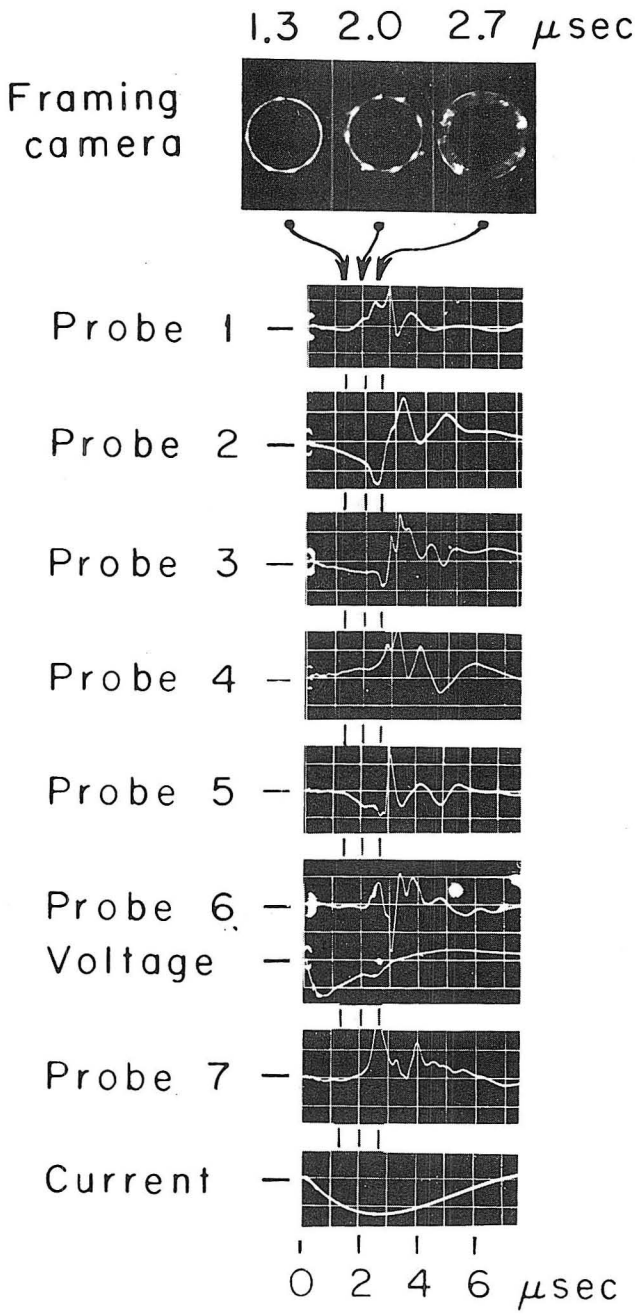
1.3 2.0 2.7 μsec
Framing camera
Probe 1
Probe 2
Probe 3
Probe 4
Probe 5
Probe 6
Voltage
Probe 7
Current
0 2 4 6 μsec
XBB 692-1459

Fig. 7

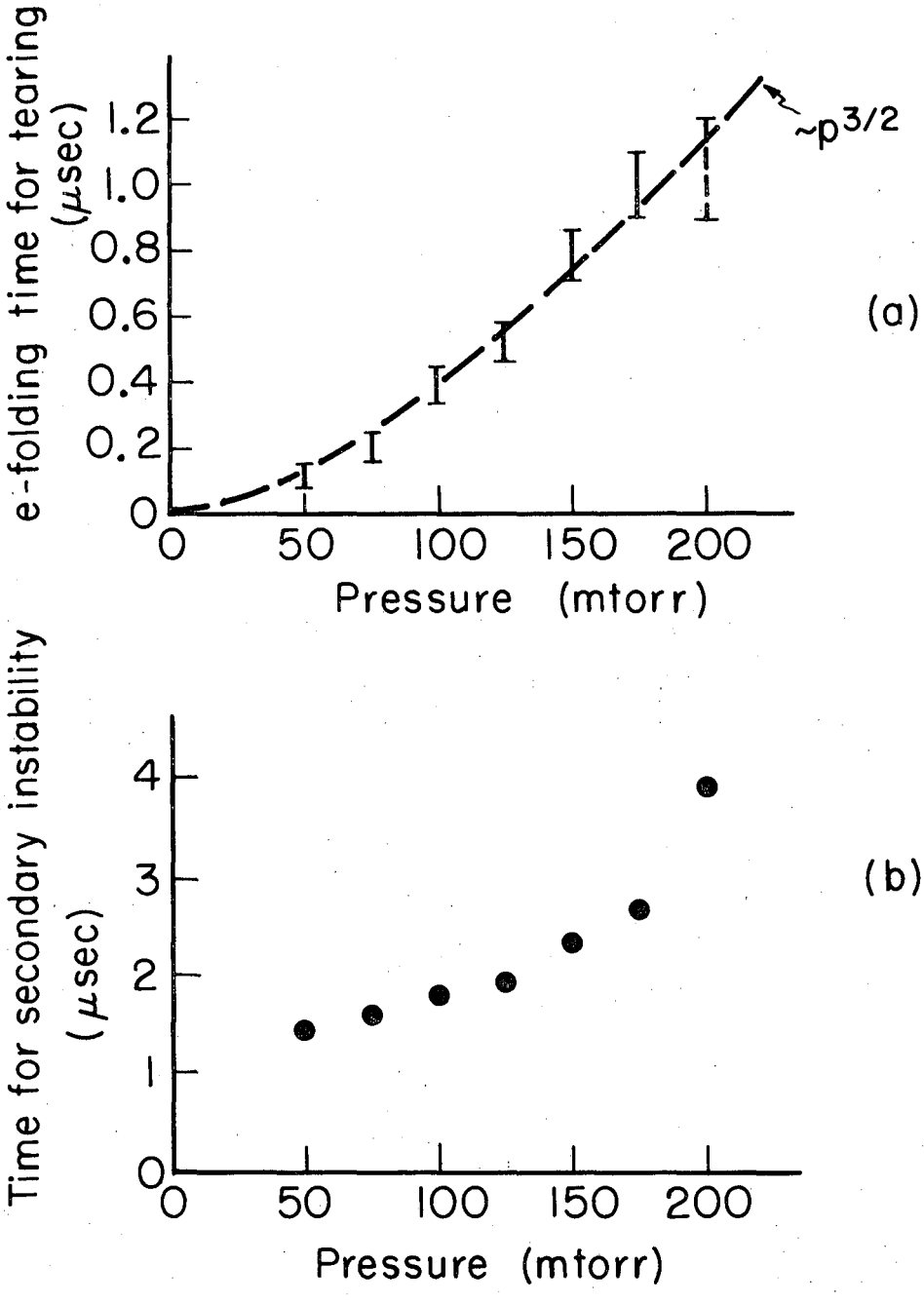
e-folding time for tearing (μsec)
1.2
1.0
0.8
0.6
0.4
0.2
0
0
50
100
150
200
Pressure (mtorr)
~p3/2
(a)
Time for secondary instability (μsec)
4
3
2
1
0
0
50
100
150
200
Pressure (mtorr)
(b)
XBL692-2064

Fig. 8

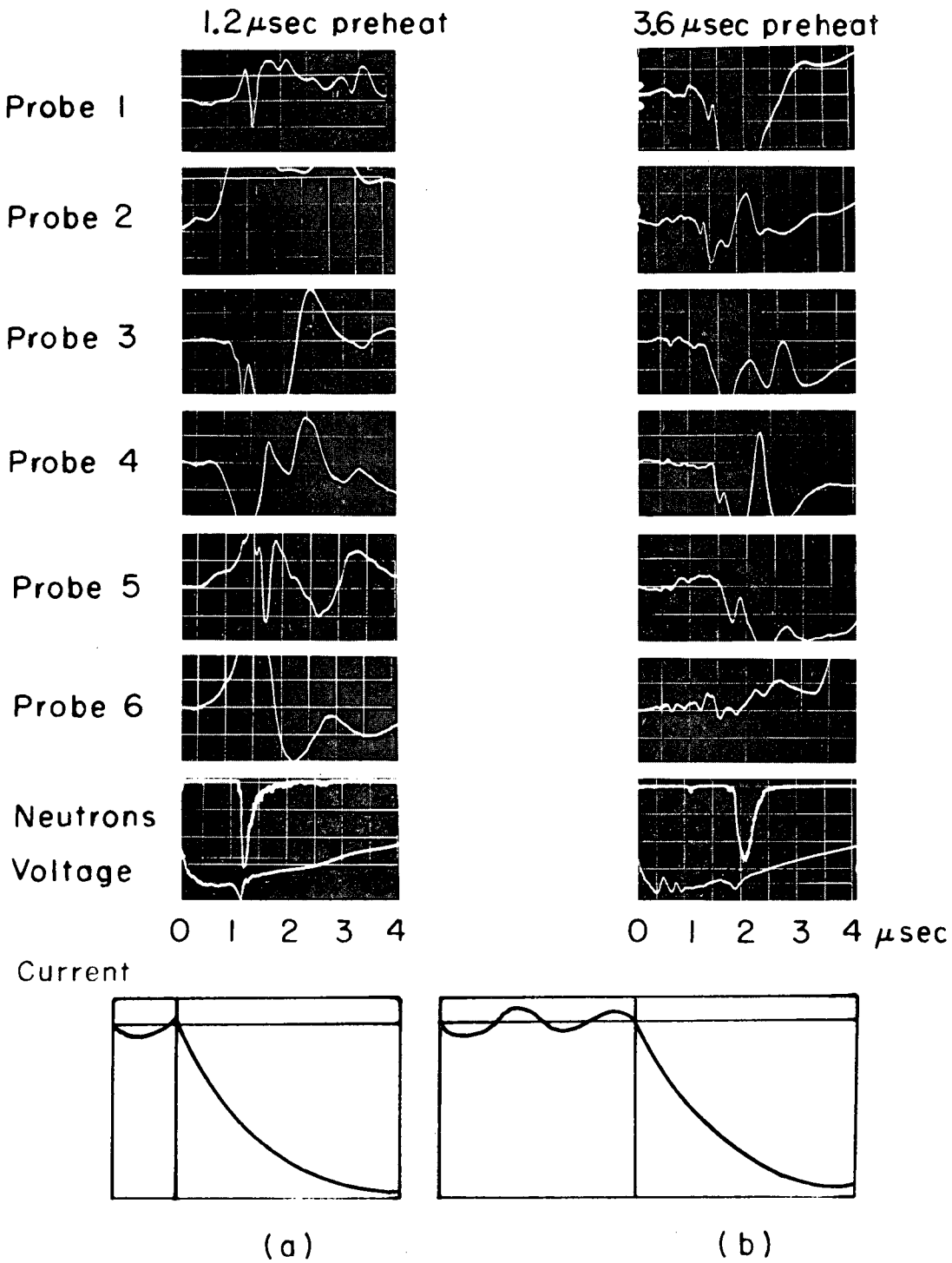
1.2 μsec preheat
3.6 μsec preheat
Probe 1
Probe 2
Probe 3
Probe 4
Probe 5
Probe 6
Neutrons
Voltage
0 1 2 3 4
0 1 2 3 4 μsec
Current
(a)
(b)
XBB 692-1460

Fig. 9

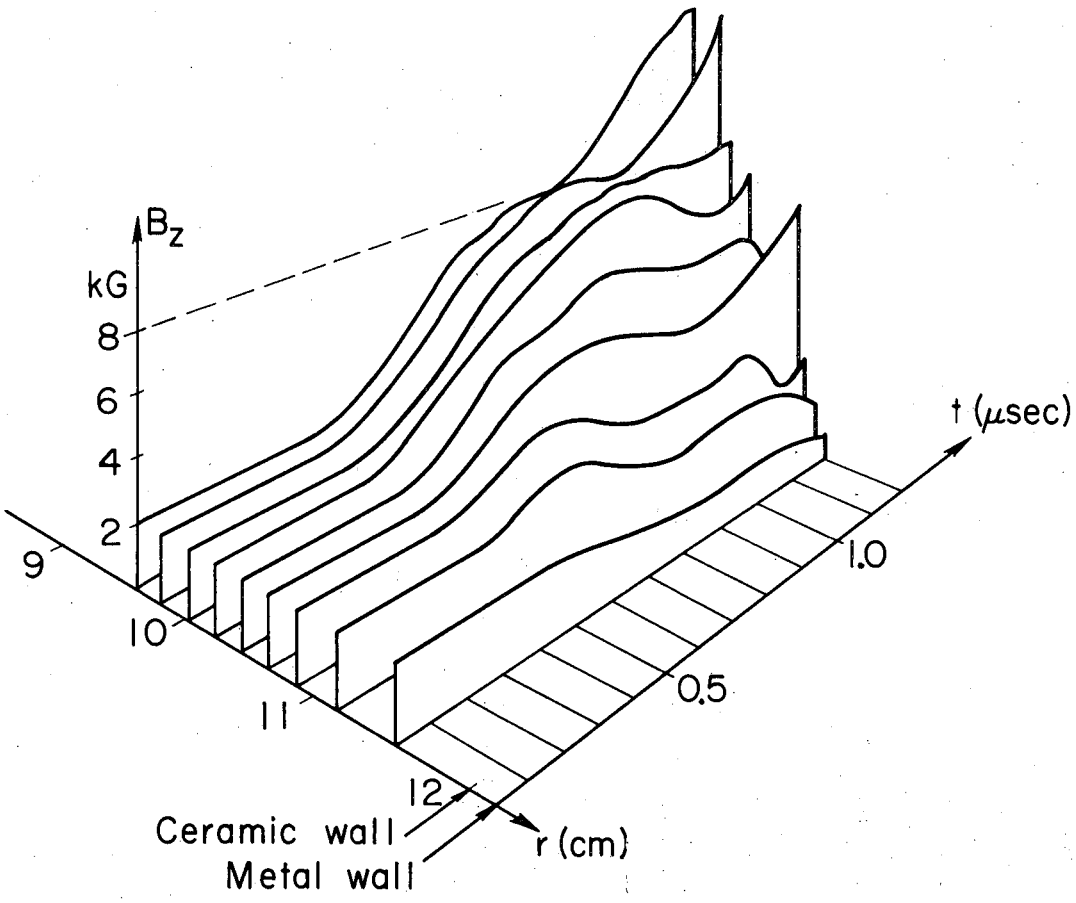

XBL692-2020

Fig. 10

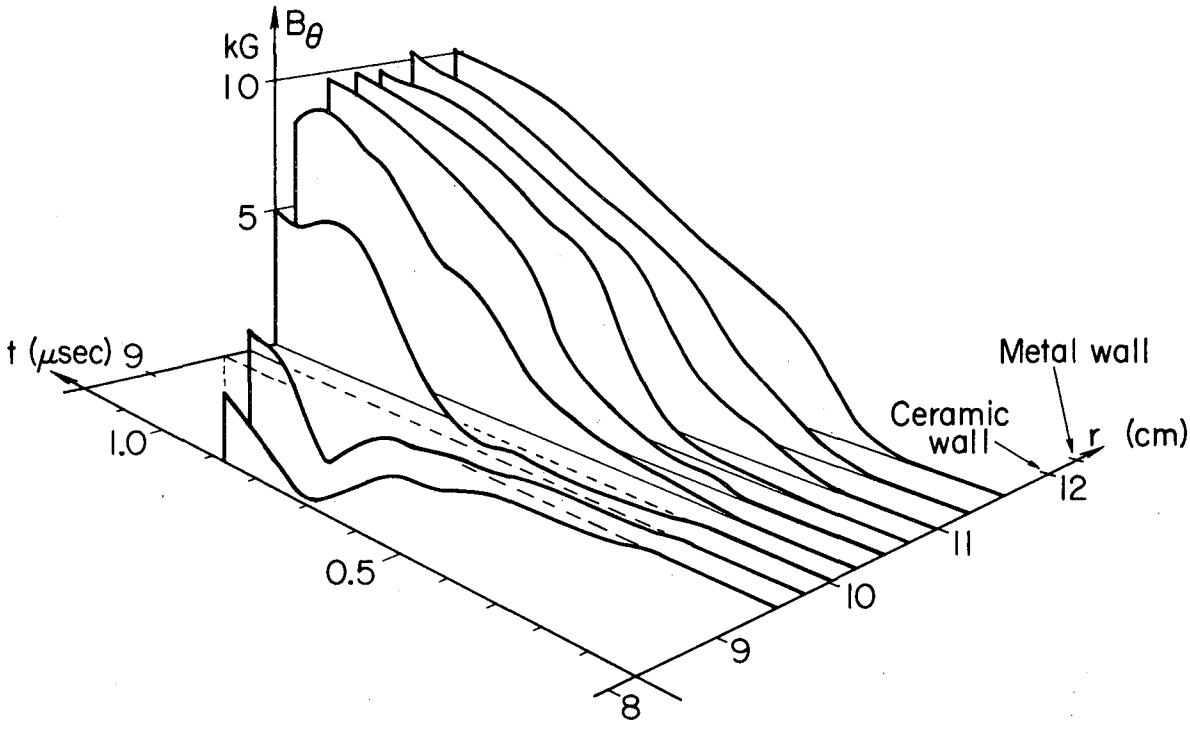

XBL692-2024

Fig. 11

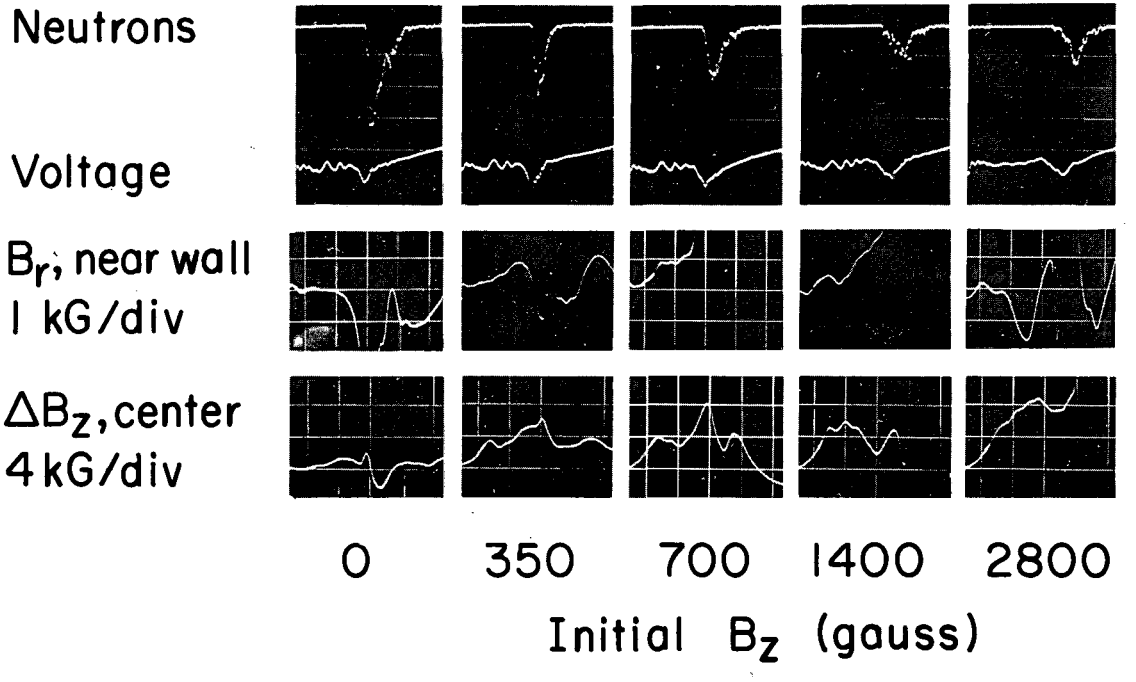

XBB 692-1347

Fig. 12

TECHNICAL INFORMATION DIVISION
LAWRENCE RADIATION LABORATORY
UNIVERSITY OF CALIFORNIA
BERKELEY, CALIFORNIA 94720